Chinese Chemical Letters 32 (2021) 5–8

Contents lists available at ScienceDirect

Chinese Chemical Letters

journal homepage: www.elsevier.com/locate/cclet

Communication

Directly conversion the biomass-waste to Si/C composite anode materials for advanced lithium ion batteries

Qiang Ma, Yu Dai, Hongrui Wang, Guozhu Ma, Hui Guo, Xianxiang Zeng, Naimei Tu*, Xiongwei Wu*, Mingtao Xiao*

College of Agronomy, School of Chemistry and Materials Science, School of Mechanical and Electrical Engineering, Hunan Agricultural University, Changsha 410128, China

ARTICLE INFO

Article history:
Received 23 September 2020
Received in revised form 1 November 2020
Accepted 3 November 2020
Available online 4 November 2020

Keywords:
Biomass-waste
Rice husks
Composite anode
Lithium ion batteries
High energy density

ABSTRACT

The necessity to explore high-efficiency and high-value utilization strategy for biomass-waste is desirable. Herein, the strategy for direct conversion biomass-waste (rice husks) to Si/C composite structure anode was built. The Si/C composite materials were successfully obtained *via* the typical thermal reduction with magnesium, and the Si nanoparticle was uniformly embedded in carbon frame, as revealed by Raman, X-ray diffraction (XRD) and transmission electron microscope (TEM) measurement. The carbon structure among rice husks was effectively used as a protective layer to accommodate the volume variation of Si anode during the repeated lithiation/delithiation process. Benefitting from the structure design, the batteries show a superior electrochemical stability with the capacity retention rate above 90% after 150 cycles at the charge/discharge rate of 0.5 C (1 C = 600 mAh/g), and hold a high charge capacity of 420.7 mAh/g at the rate of 3 C. Therefore, our finding not only provides a promising design strategy for directly conversion biomass-waste to electrochemical storage materials but broadens the high-efficiency utilization method for other biomass by-products.

Rice one of the most crop species is planting spread all over the world. In recent years, large amount of rice has been needed to meet the demand for the living life of increasing population of the world [1]. Huge amount of rice husks (RHs) by-product was concomitantly produced, which is an environmental nuisance giving rise to severe stress for global environment [2]. However, the applications for RHs have suffered from the dilemma of low added value, such as fertilizer additives, stockbreeding rugs, fuels, and landfilling or paving materials. Hence, exploring high-efficiency and high-value utilization strategy for RHs is desirable and in accord with the policy of the global sustainable development [3–5].

Lithium ion batteries regarded as a green electrochemical storage technology are widely used in our daily life such as cell phone, computer and electric vehicle [6,7]. Meanwhile, graphite as the most intriguing anode materials has awarded much more attention since their commercialization by Sony. In recent years, a wide range of modification strategies have been used to improve the capacity of graphite [8,9], which nearly reached the peak of their theoretical capacity and could not be improved [10,11]. Pursuing for high energy density and long-range endurance mileage, it is significant to explore anode materials with higher capacity to replace the currently used graphite anode [12–15].

Silicon as the promising anode materials with the ultrahigh theoretical capacity ($Li_{15}Si_4$, 3580 mAh/g) has made much attention in the field of electrochemical energy storage [16,17]. However, suffering from inferior cycling stability for silicon anode is a major reason to limit their further development because of the tremendous volume variation, up to 300% during lithiation /delithiation process, which makes the electrode materials crack and loss the electrical contact in bulk electrode [18–21]. Besides, continuously consume lithium ion to form fresh solid electrolyte interphase (SEI) for cracking electrode is another issue to lead the fading of the capacity and calendar life [22–25]. Therefore, extensive efforts have been devoted to ameliorate the above-mentioned issues in order to stabilize the structure of anode materials and ensure the available electrical contact among electrode materials [26–29]. The development of Si/C composite structure is an effective strategy, in which nano/micro Si nanoparticle embedded in the C skeleton could accommodate the volume change during the lithiation/delithiation process and provide effective electron transfer pathway [30–34]. The commonly used method to derive the Si/C compounds is electrostatic

* Corresponding authors.
E-mail addresses: tnm505@163.com (N. Tu), wxwcsu05@aliyun.com (X. Wu), xiaomentor@163.com (M. Xiao).

https://doi.org/10.1016/j.cclet.2020.11.007

spinning, ball milling and spray drying [35,36]. Nevertheless, the derived compounds could not ensure the nano/micro Si uniformly mingle with the C protective skeleton. The facile and effective method to obtain Si/C composite materials is urgently needed to meet the demands of rapid growth hybrid electrical vehicles and portable electronic devices [37–39]. The recent pioneer works have proved that high amounts of silica in the form of nanoparticle was possessed in RHs, meanwhile the nanosized Si particle was reduced from silica, then mixed with carbon nanotube or graphene to construct Si/C composite structure [40]. However, the naturally existed carbon matrix among RHs were destructed and unavoidably it could impact the naturally composite structure.

Herein, the strategy for direct conversion biomass-waste (rice husks) to Si/C composite structure anode was built. The Si/C composite materials was successfully obtained *via* the typical thermal reduction with magnesium, and the Si nanoparticle was uniformly embedded in carbon frame, as revealed by Raman, XRD and TEM measurement. The carbon bulk among rice husks was effectively used as the protective layer to accommodate the volume variation of Si anode during the repeated lithiation/delithiation process.

The R-Si/C composite anode was fabricated based on the route of Fig. 1. Firstly, the RHs were collected from rice plants (RPs) at the mature stage, which was treated at 105 °C for 24 h to eliminate the moisture among the materials. Then, the treated RHs was directly carbonized at 900 °C to obtain the precursor of rice husk derived carbon (R-C). Finally, the typical magnesiothermic reduction strategy was adopted to convert the R-C precursor to the hybrid anode materials of rice husk derived Si/C (R-Si/C) under Ar inert atmosphere at the temperature of 680 °C for 3 h, and the morphology variation for electrode materials from R-C to R-Si/C was shown in Fig. S1 (Supporting information). The TEM measurement was carried out to investigate the internal structure of R-C and R-Si/C (Fig. 2a). In comparison with the typical amorphous form of R-C (Fig. S2 in Supporting information) and crystal structure of nano-Si (Fig. S3 in Supporting information), some nano Si crystalline regions with the size of 20 nm were observed among R-Si/C electrode materials, as displayed in Figs. 2b and c. Meanwhile, it is effectively to utilize the intrinsic carbon structure of rice husk without additional carbon source introducing to preparation process. Furthermore, the carbon structure as a protective layer uniformly wrapped the reduction Si nanoparticles (Si NPs), which could mitigate the volume variation during the repeated lithiation/delithiation process. The carbon substrate and Si nanodomains were clearly shown in Figs. 2d and e, and the

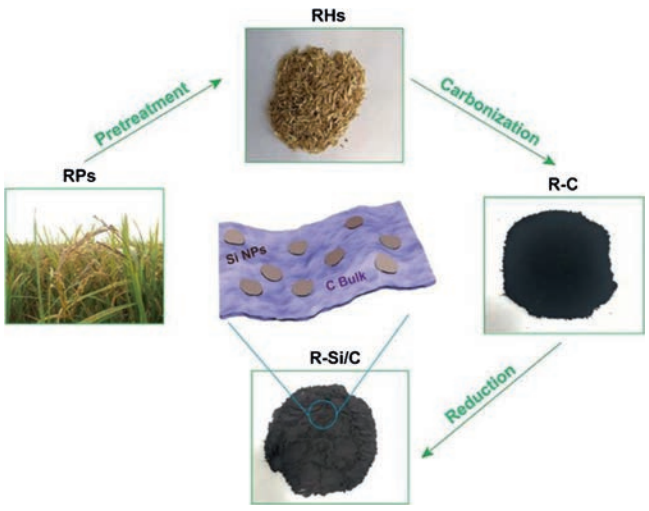

Fig. 1. Schematic illustration for the synthesis of R-Si/C composite anode.

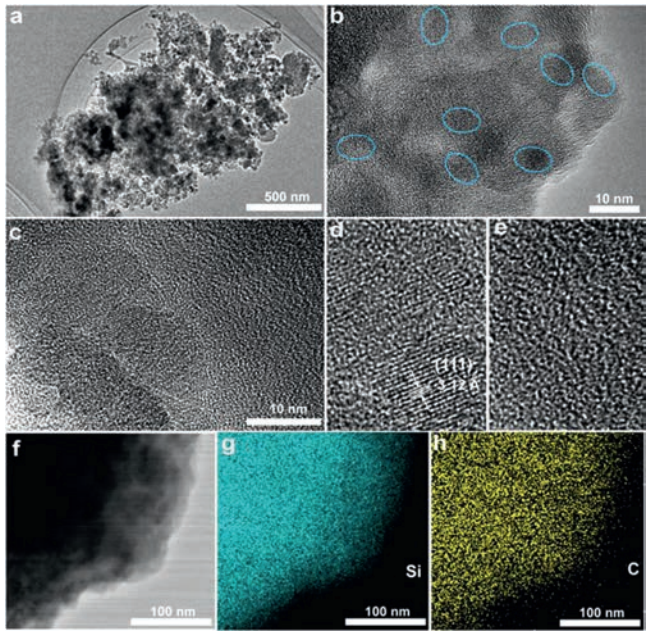

Fig. 2. (a) The TEM image and (b, c) high-resolution TEM images of R-Si/C. Details information for R-Si/C (d) Si and (d) C region; (f) TEM image and corresponding EDS mapping for (g) Si and (h) C element.

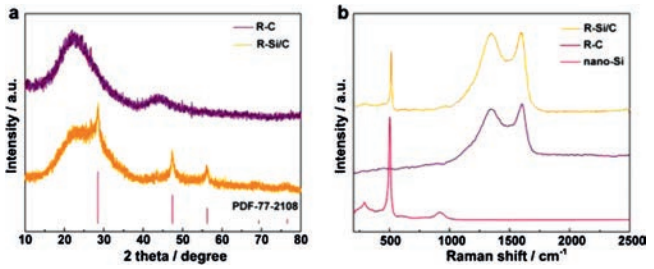

Fig. 3. (a) The XRD curves of R-Si/C and R-C. (b) The typical Raman spectra of R-Si/C, R-C and nano-Si.

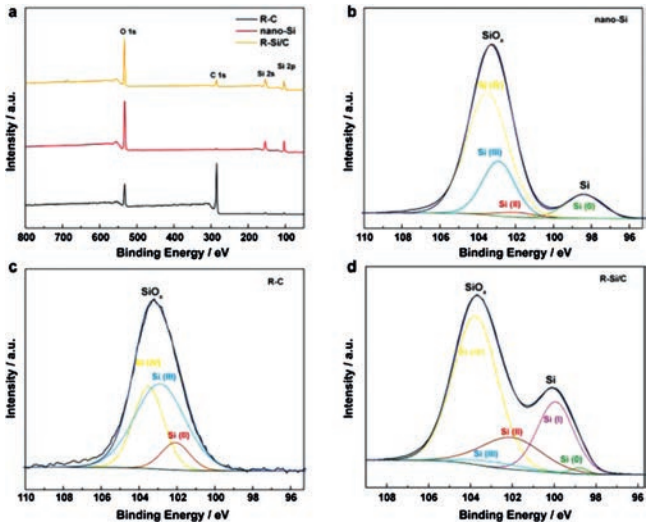

Fig. 4. (a) The XPS survey of R-C, nano-Si and R-Si/C materials. The XPS result for the surface message of (b) nano-Si, (c) R-C and (d) R-Si/C.

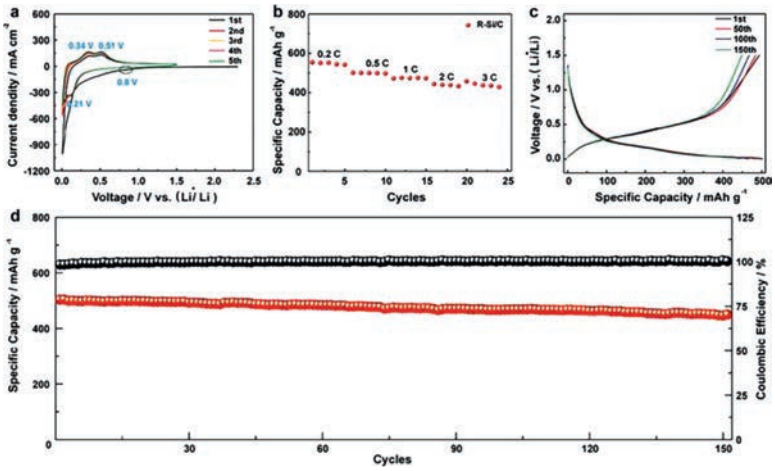

Fig. 5. (a) The CV curves of R-Si/C during the lithiation /delithiation process with a scan rate of 0.1 mV/s. (b) The rate performance result of R-Si/C with the charge rate ranging from 0.2 C to 3 C. (c) The cycling test profiles and (d) corresponding stability result at the rate of 0.5 C.

interplanar spacing is 0.312 nm corresponding to the (111) crystalline plane (PDF-77-2108) [41]. The energy dispersive spectroscopy (EDS) result shows that the Si and O elements are homogeneously distributed among composite anode, as presented in Figs. 2f–h.

Additionally, the further demonstration of R-Si/C composite structure was revealed by XRD and Raman spectrum analysis. The typical amorphous XRD pattern for R-C was obtained as seen from Fig. 3a. Different from the R-C materials, the signals of amorphous carbon and silicon grain were also contained in R-Si/C, indicating that the composite electrode was successfully converted from biomass-waste, which was in accord with the result of TEM. The peak located at 518 cm^{-1} belongs to the Si characteristic peak, and the other peaks located at 1352 and 1598 cm^{-1} are attributed to the typical D band and G band of carbon, respectively (Fig. 3b) [42]. According to the Raman spectrum of separated nano-Si and R-C, it also could be seen that the Si characteristic peak and the typical D band and G band belonging to the nano-Si and R-C were detected, respectively. The X-ray photoelectron spectroscopy (XPS) was employed to investigate the surface condition of R-C, nano-Si and R-Si/C. The signals locating at 103.1 and 154.6 eV are attributed to the Si 2p and Si 2s, respectively (Fig. 4a). Meanwhile, the Si 2p peak could be de-convoluted into five valence states: Si(0), Si(I), Si(II), Si(III) and Si(IV), as shown in the Figs. 4b–d. In comparison with the Si 2p signal of R-C materials, the signals of Si(0) and Si(I) were observed from R-Si/C and nano-Si materials respectively [43,44], further demonstrating that the Si NPs was successfully converted from silica among R-C with the method of magnesiothermic reduction, which is consistent with the results of TEM, XRD and Raman measurement.

The cyclic voltammetry (CV) test was conducted to evaluate the electrochemical behavior of R-Si/C anode materials during lithiation/delithiation process. The irreversible broad cathodic peak centered at 0.8 V corresponds to the formation of SEI at the first cycle [45–47], which is in accordance with the result of electrochemical impedance (Fig. S4 in Supporting information). In addition, the cathodic peak at 0.21 V was ascribed to the lithiation process of Si, while the other two anodic peaks located at 0.34 V and 0.51 V originated from the delithiation reaction of Li_xSi alloy (Fig. 5a) [48]. After the first cycle, the subsequent profiles were stable, indicating that the activation process is completed. The Li|| Si half battery was used to further measure the rate performance of R-Si/C with the rate ranging from 0.2 C to 3 C (Fig. 5b). The result shows that the R-Si/C exhibit a superior rate performance with the charge capacity of 540.3 and 420.7 mAh/g at the rate of 0.2 and 3 C, respectively (Fig. S5 in Supporting information). Furthermore, the charge and discharge capabilities of R-Si/C was also compared with the R-C and commercial graphite anode. The R-Si/C composite anode with the charge capacity of 501.4 mAh/g at 0.5 C is much higher than that of R-C and commercial graphite anode materials, which could exert the charge capacity of 344.2 and 365.3 mAh/g, respectively (Figs. S6 and S7 in Supporting information), meaning that the biomass derived Si/C composite anode materials hold the promising of usage in high energy density batteries type. The result of cycling stability for R-Si/C composite anode was displayed on Fig. 5d. An excellent cycling stability for R-Si/C anode with the capacity retention above 90% was acquired.

In summary, we have successfully established a strategy for direct conversion biomass-waste (rice husks) to Si/C composite structure anode. The Si/C composite materials were successful obtained *via* the typical thermal reduction with magnesium, and the Si nanoparticle was uniformly embedded in carbon frame, as revealed by Raman, XRD and TEM measurement. The carbon structure among rice husks was effectively used as a protective layer to accommodate the volume variation of Si anode during the repeated lithiation/delithiation process. Thanks to the structural design, the batteries with Si/C composite anode show a superior electrochemical stability with the capacity retention rate above 90% after 150 cycles at the charge/discharge rate of 0.5 C (1 C = 600 mAh/g), and hold a high charge capacity of 420.7 mAh/g at the rate of 3 C. Therefore, our finding not only provides a promising design strategy for directly conversion biomass-waste to electrochemical storage materials but broadens the high-efficiency utilization method for other biomass by-products.

Declaration of competing interest

The authors report no declarations of interest.

Acknowledgments

The National Natural Science Foundation of China (Nos. 51803054, 51772093), the Natural Science Foundation of Hunan province (Nos. 2019JJ20010, 2020JJ3022, 2019JJ50223), the

"Double first-class" School Construction Project (No. SYL201802008) and Outstanding Youth Foundation (No. 19B270) from Education Department of Hunan Province.

Appendix A. Supplementary data

Supplementary material related to this article can be found, in the online version, at doi:https://doi.org/10.1016/j.cclet.2020.11.007.

References

[1] N. Liu, K. Huo, M.T. McDowell, et al., Sci. Rep. 3 (2013) 1919.
[2] A. Xing, S. Tian, H. Tang, et al., RSC Adv. 3 (2013) 10145–10149.
[3] D.S. Jung, M.H. Ryou, Y.J. Sung, et al., Proc. Natl. Acad. Sci. 110 (2013) 12229–12234.
[4] W. Long, B. Fang, A. Ignaszak, et al., Chem. Soc. Rev. 46 (2017) 7176–7190.
[5] J. Chen, Z. Mao, L. Zhang, et al., ACS Nano 11 (2017) 12650–12657.
[6] M. Armand, J.M. Tarascon, Nature 451 (2008) 652–657.
[7] M. Winter, B. Barnett, K. Xu, Chem. Rev. 118 (2018) 11433–11456.
[8] Y. Wang, W. Tian, L. Wang, et al., ACS Appl. Mater. Interfaces 10 (2018) 5577–5585.
[9] H. Tao, S. Du, F. Zhang, et al., ACS Appl. Mater. Interfaces 10 (2018) 34245–34253.
[10] Z. Yan, Q.W. Yang, Q. Wang, et al., Chin. Chem. Lett. 31 (2020) 583–588.
[11] M. Li, J. Lu, Z. Chen, et al., Adv. Mater. 30 (2018) e1800561.
[12] G. Li, L.B. Huang, M.Y. Yan, et al., Nano Energy 74 (2020) 104890.
[13] F. Luo, B. Liu, J. Zheng, et al., J. Electrochem. Soc. 162 (2015) A2509–A2528.
[14] Q. Xu, J.K. Sun, Y.X. Yin, et al., Adv. Funct. Mater. 28 (2017) 1705235.
[15] X. Xie, S. Qi, D. Wu, et al., Chin. Chem. Lett. 31 (2020) 223–226.
[16] T. Munaoka, X. Yan, J. Lopez, et al., Adv. Energy Mater. 8 (2018) 1703138.
[17] T. Liu, Q. Chu, C. Yan, et al., Adv. Energy Mater. 9 (2018) 1802645.
[18] D. Vrankovic, M. Graczyk-Zajac, C. Kalcher, et al., ACS Nano 11 (2017) 11409–11416.
[19] N. Kim, H. Park, N. Yoon, et al., ACS Nano 12 (2018) 3853–3864.
[20] Y. Zhu, W. Hu, J. Zhou, et al., ACS Appl. Mater. Interfaces 11 (2019) 18305–18312.
[21] X. Yang, Y.Y. Wang, B.-H. Hou, et al., Acta Metall. Sin. (Engl. Lett.) (2020), doi: http://dx.doi.org/10.1007/s40195-020-01001-7.
[22] S.H. Kim, Y.S. Kim, W.J. Baek, et al., ACS Appl. Mater. Interfaces 10 (2018) 24549–24553.
[23] R. Reinhold, U. Stoeck, H.J. Grafe, et al., ACS Appl. Mater. Interfaces 10 (2018) 7096–7106.
[24] Y. Jin, N.J.H. Kneusels, L.E. Marbella, et al., J. Am. Chem. Soc. 140 (2018) 9854–9867.
[25] M. Haruta, T. Okubo, Y. Masuo, et al., Electrochim. Acta 224 (2017) 186–193.
[26] H. Wu, G. Chan, J.W. Choi, et al., Nat. Nanotech. 7 (2012) 310–315.
[27] H.J. Kwon, J.Y. Hwang, H.J. Shin, et al., Nano Lett. 20 (2020) 625–635.
[28] D.P. Wong, R. Suriyaprabha, R. Yuvakumar, et al., J. Mater. Chem. A 2 (2014) 13437–13441.
[29] Y.Y. Wang, B.H. Hou, J.Z. Guo, et al., Adv. Energy Mater. 8 (2018) 1703252.
[30] J. Yu, H. Zhan, Y. Wang, et al., J. Power Sources 228 (2013) 112–119.
[31] Z. Zhou, L. Pan, Y. Liu, et al., Chin. Chem. Lett. 30 (2019) 610–617.
[32] C. Shan, K. Wu, H.J. Yen, et al., ACS Appl. Mater. Interfaces 10 (2018) 15665–15672.
[33] F. Zhao, X. Zhao, B. Peng, et al., Chin. Chem. Lett. 29 (2018) 1692–1697.
[34] Y.B. An, S. Chen, M.M. Zou, et al., Rare Met. 38 (2019) 1113–1123.
[35] S. Basu, S. Suresh, K. Ghatak, et al., ACS Appl. Mater. Interfaces 10 (2018) 13442–13451.
[36] I.K. Ahn, Y.J. Lee, S. Na, et al., ACS Appl. Mater. Interfaces 10 (2018) 2242–2248.
[37] Q. Chen, H. Zheng, Y. Yang, et al., ChemSusChem 12 (2019) 252–260.
[38] T. Wang, X. Guo, H. Duan, et al., Chin. Chem. Lett. 31 (2020) 654–666.
[39] C. Wei, H. Fei, Y. Tian, et al., Chin. Chem. Lett. 31 (2020) 980–983.
[40] Y.C. Zhang, Y. You, S. Xin, et al., Nano Energy 25 (2016) 120–127.
[41] G. Li, J.Y. Li, F.S. Yue, et al., Nano Energy 60 (2019) 485–492.
[42] M. Aghajamali, H. Xie, M. Javadi, et al., Chem. Mater. 30 (2018) 7782–7792.
[43] Z. Zhang, Y. Wang, W. Ren, et al., Angew. Chem. Int. Ed. 53 (2014) 5165–5169.
[44] J. Deng, H. Ji, C. Yan, et al., Angew. Chem. Int. Ed. 52 (2013) 2326–2330.
[45] Y. Jin, B. Zhu, Z. Lu, et al., Adv. Energy Mater. 7 (2017) 1700715.
[46] T. Xu, Q. Wang, J. Zhang, et al., ACS Appl. Mater. Interfaces 11 (2019) 19959–19967.
[47] H. Liu, Z. Shan, W. Huang, et al., ACS Appl. Mater. Interfaces 10 (2018) 4715–4725.
[48] B.M. Koo, D.A.D. Corte, J.N. Chazalviel, et al., Adv. Energy Mater. (2018) 1702568.